Bull. Spec. Astrophys. Obs., 1997, 43, 95–108

The structure of the supercritical accretion disk of SS 433

S.N. Fabrika[a], A.A. Panferov[a], L.V. Bychkova[a], V.Yu. Rakhimov[b]

[a] Special Astrophysical Observatory of the Russian AS, Nizhnij Arkhyz 357147, Russia
[b] Institute of Astrophysics, Dushanbe, 734042, Tadzhikistan

Received March 21, 1997; accepted May 15, 1997.

Abstract. The results are presented of spectral and photometrical Hα observations of SS 433 carried out in the accretion disk eclipses. It is found that He II emission is formed in the accretion disk area and consists of two components — a narrow Gaussian profile with FWHM $\approx$ 1000 km/s and a broad double–peaked profile. The emission regions of the narrow He II line and hydrogen Hβ and Hα lines are partially eclipsed at orbital phases 0.1 for He II and 0.1–0.2 for hydrogen lines Hβ and Hα. This indicates that these lines are emitted in a gas stream directed to the accretion disk. Radial velocity half–amplitudes of the stream–formed emissions are K $\approx$ 80 km/s. An electron scattering is probably responsible for these lines broadening. The broad double–peaked He II line is totally eclipsed at phase 0.0. Its blue and red peaks are probably emitted in gas cocoons around the relativistic jet bases. The gas outflow velocity in the cocoons is $\approx$ 1500 km/s. The He II cocoon size is 0.25–0.30 measured in units of orbital radius. Inside the cocoon the X–ray emitting region is situated, whose size is 0.2. The red He II cocoon is not eclipsed by the accretion disk body, but it is totally eclipsed by the optical star.

Key words: stars: close binary: individual (SS 433) — accretion disk — jet

1. Introduction

SS 433 is a unique binary system in which gas is accreted by the relativistic companion under a supercritical regime. In the accretion disk there formed two opposite jets which spread at a velocity of 0.26 that of light. The jets precess with a period of $162^{d}.5$. The mean brightness of the system varies with the same period. Besides, SS 433 shows itself as an eclipsing binary with a period of $13^{d}.082$. Eclipses have been observed in the optics and X–rays. A detailed description of the SS 433 light curve can be found in Gladyshev et al. (1987). The radial velocity curves of the stationary emission lines H and He show the orbital modulation as well (Crampton, Hutchings, 1981; Kopylov et al., 1989). The source of the He II λ4686 emission line is located in the upper conjunction at the phase of the primary minimum (Gladyshev et al., 1983) — the phase of eclipse of the accretion disk.

Shakura (1972), van den Heuvel et al. (1980) have suggested a model of a precessing or "slaved" accretion disk. This explains the brightness variability of SS 433 with the precession period: the system becomes brighter with increasing projection area onto the sky plane. Precession of the disk axis results from precession of the massive OB star rotational axis, which is oblique to the orbital axis. However, so far there has been no unified model that could fully explain orbital and precession light curves. The data of the optical and X–ray observations suggest that the bright source (accretion disk), which is eclipsed at the primary minimum, is rather a multicomponent one as is the case in cataclysmic variables. The source complexity may be due to several factors. There are grounds to believe (Lipunov, Shakura, 1982; Fabrika, 1984) that at the place of the jet emergence there are hot spots on the accretion disk. Besides, the gas stream and the spot on the disk rim, where the stream strikes the disk, may contribute significantly to the luminosity of the source. The conditions for the disk visibility change in the course of precession, which has influence on the shape of eclipses and light curves as a whole.

In the system SS 433 the optical star overfills its

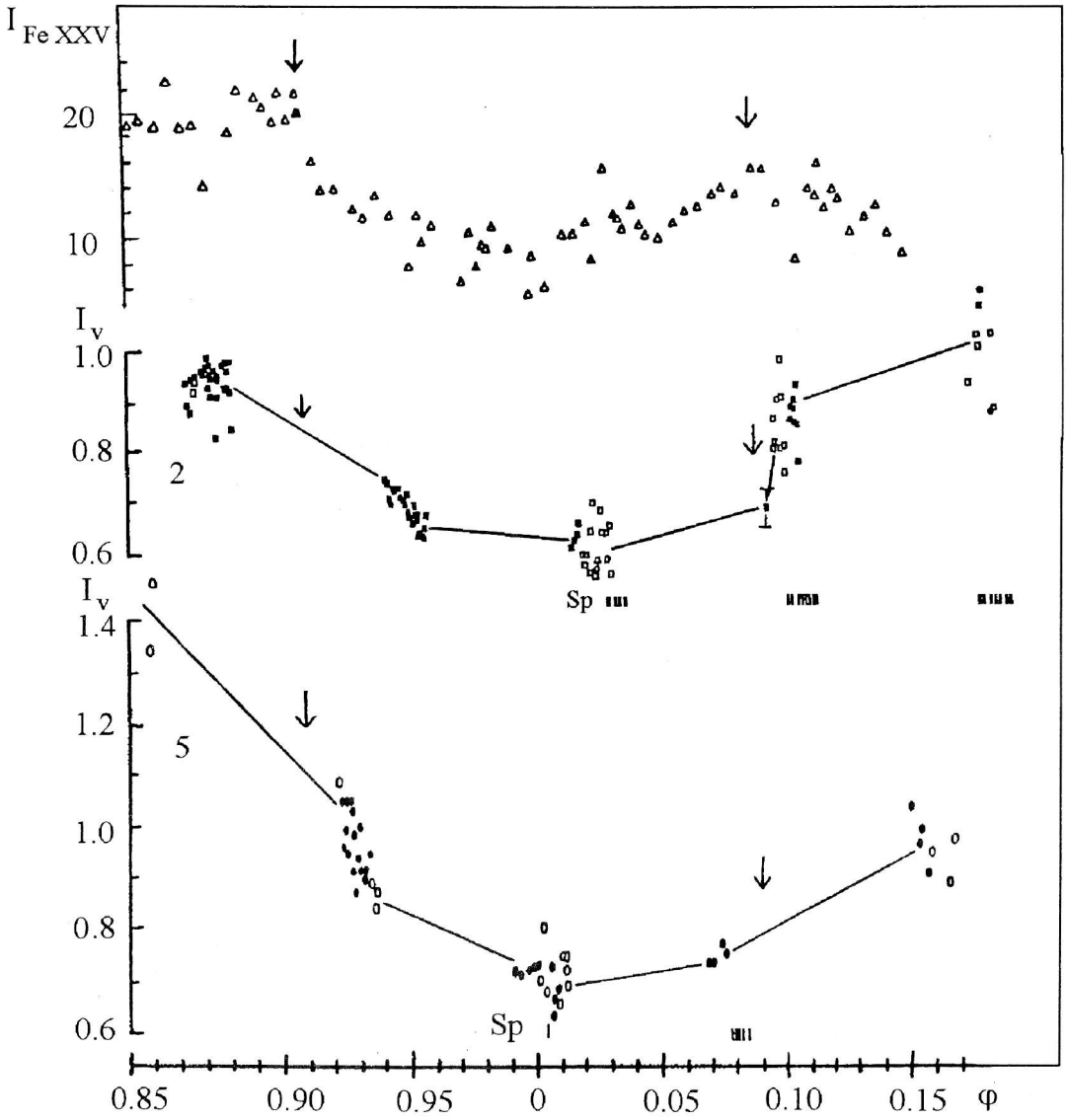

Figure 1: *Eclipse light curves of SS 433 in the V band and X-rays. Top — the Fe XXV emission line intensity from Ginga (Kawai et al., 1989), middle — eclipse on June 1–5, 1986, bottom — eclipse on September 2–5, 1988. Open symbols — photographic observations, filled - photoelectric. Vertical lines show the phases of spectral observations*

critical Roche lobe and supplies about 10^{-4} $M_\odot$/y to the accretion disk around the relativistic star (Shklovskij, 1981; Van den Heuvel, 1981). As a result of this a supercritical accretion disk is formed, from which nearly all this gas flows out. The structure of such a disk is of great interest. Goranskij et al. (1987) have shown that the regions of formation of the stationary lines of SS 433 are eclipsed by the optical star. Analysis of the behaviour of the radial velocities and profiles of those lines may provide information on the accretion disk structure. In the present paper we study the structure of the disk in the lines He II λ4686 and Hβ. We use the data of the spectral observations carried out during the eclipses of June 1–5, 1986 (eclipse 1, precession phase $\psi = 0.92$) and September 2–5, 1988 (eclipse 2, $\psi = 0.99$). These observations are part of the long-term programme of monitoring eclipses in SS 433. Additional information

about this programme, in particular, about the photometry data of SS 433 can be found in (Goranskij et al., 1997; Fabrika et al., 1997 b).

2. Photometric behaviour of SS 433 in eclipses

During the eclipses considered herein photometric observations of the object were also carried out. Here we use the main results of the photometry of SS 433 obtained during these eclipses and described in (Goranskij et al., 1997), and we also present new results regarding the object behaviour in Hα. Our observations refer to precession phases near $\psi = 0$, i. e. when the disk projection onto the sky plane is maximal. At these precession phases from the orbital phase $\varphi = 0.75$ to the first contact at $\varphi = 0.9$ the system's brightness gradually decreases by about 25 % in the V band, then it drops abruptly. The phases of contacts as well as the rate of rise and decrease of brightness are apparently varied depending on the precession phase (even in a narrow interval of phases, $0.9 < \psi < 0.1$), i. e. on the orientation of the disk. The slow brightness variations between the contacts and elongations may be both the consequence of the optical star heating and eclipse of the outer parts of the accretion disk.

In Fig. 1 the V–band fluxes of SS 433 in the eclipses under discussion (Goranskij et al., 1997) are displayed. The out–of–eclipse brightness $V = 14\overset{m}{.}0$ is taken as a unit. Before the eclipse of 1988 a flare occurred during which the brightness rose by 40 % above the quiet average level, and the eclipse began in the active state. The descending branch of this eclipse and the level of the bottom are well above the quiet state level and are gradually approaching it. The amplitude of sudden drops and rises of the brightness at ingress and egress phases amounts to almost $0\overset{m}{.}3$. In the figure is presented the Fe XXV emission line intensity curve obtained in Ginga observations during the eclipse of May 18–23, 1987 ($\psi = 0.09$) (Kawai et al., 1989). As it is known the eclipse in the X–rays is partial and makes up about 50 % of the total intensity. From our data it can be concluded (Goranskij et al., 1997) that the outer contacts in the X–ray eclipse coincide with the contacts in optics. Hence the bright optical source is a region around the X–ray jet.

In Fig. 2 the light curves and colour indices are presented from the data of Goranskij et al. (1997) at the primary minima of the eclipses. It follows from the figure that with the brightness decrease the colour indices increase considerably on the average (but in each individual eclipse the light curves have a particular shape). The amplitude of the flux variations is maximal in the U band and decreases with the wavelength, i. e. the hotter source of radiation is eclipsed.

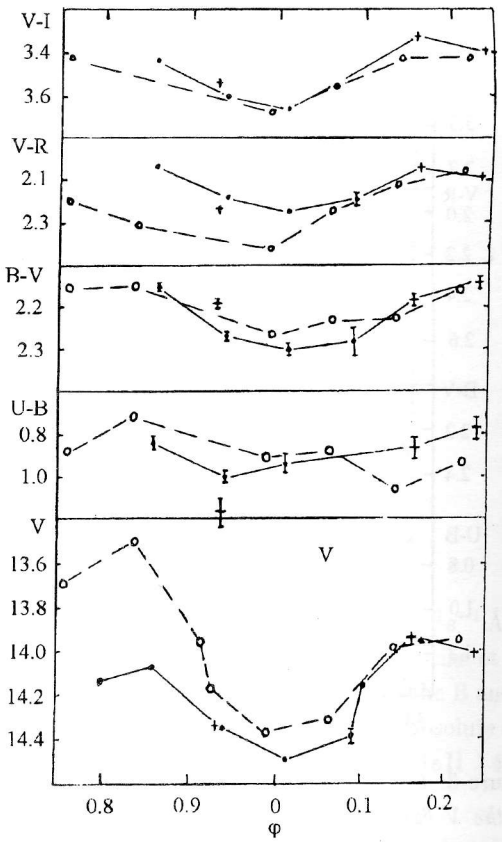

Figure 2: *The light curves and colour indices at the primary minimum. Circles — eclipse of 1988, dots — 1986, crosses — the following orbital cycle after this eclipse. The measurement errors are shown by vertical bars in cases when the errors are larger than the symbol sizes in the figure*

In Fig. 3 the relationships between the colour indices and the V band fluxes are presented from the data obtained in the frames of the co-operative observing programs in 1986–1988. The data refer to the precession phase $0.9 < \psi < 0.1$. In the range $14\overset{m}{.}0 < V < 14\overset{m}{.}6$ the colour indices increase almost linearly with increasing brightness, which is due to eclipse of the hot source. In the range $V \leq 13\overset{m}{.}9$ the colour indices (V–R) and (V–I) begin to increase, while the colour indices (U–B) and (B–V) remain approximately unchanged. This suggests that in the blue and yellow regions the spectrum of flares is similar to that of the object in elongations. In the red part of the spectrum an additional emission appears during flares. In the course of powerful flares (at

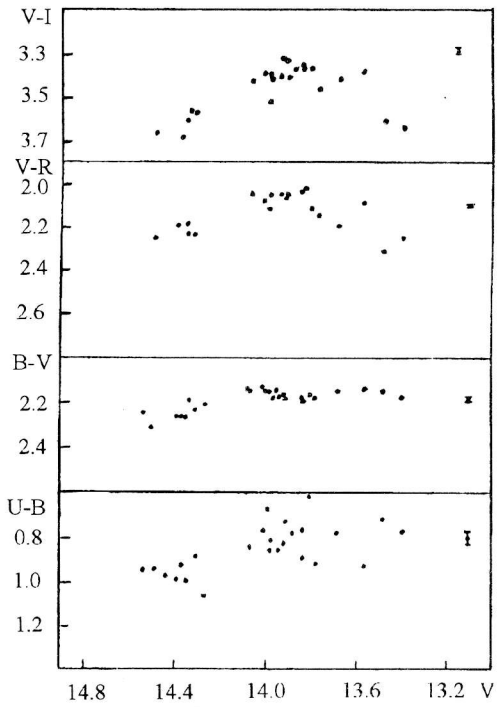

Figure 3: *Colour indices as a function of brightness in the V band, for precession phases* $0.9 < \psi < 0.1$ *(average points). Errors* $\pm\sigma$ *are shown right.*

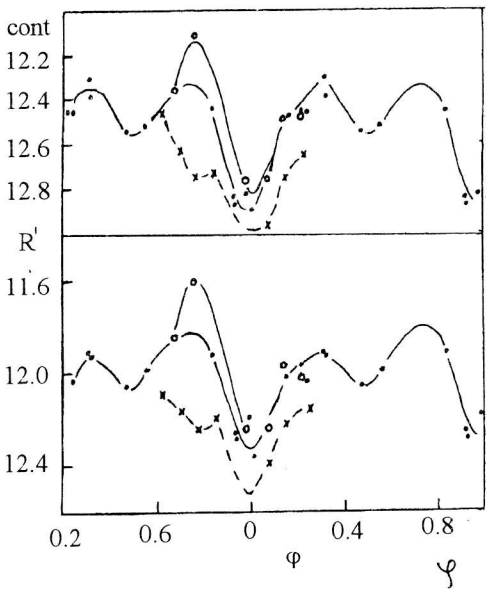

Figure 4: *The light curves in the R′ band and the "cont" band (R and S bands after subtraction of radiation contribution in* Hα*). Circles — eclipse of 1988, dots — 1986 and the following orbital cycle. Crosses show the data at the precession phase* $\psi = 0.7 \div 0.8$.

$V < 13\overset{m}{.}8$ as follows from Fig. 3) the UV radiation may ionize the surrounding envelope, which may cause the R and I band fluxes to rise.

Recently Dolan et al. (1997) have found that in the R band even in the quiet state of the object there exists an additional (apparently free–free) radiation. When analysing the spectrum of SS 433 from the UV (the Space Telescope data) to the R band they have found the spectrum to be in good agreement with that of a single blackbody source whose temperature T $\approx$ 60000 K, the interstellar absorption being $A_V = 8\overset{m}{.}0 - 8\overset{m}{.}2$. The additional emission contributes to the R band about 30–50 % depending on the phase of precession. No variability of this additional radiation either with precession or orbital phases has been detected; that is why Dolan et al. (1997) assumed that this is the emission of a gas that surrounds the binary system. With a reduction of the system's flux at other precession phases, the curve (V–R) is displaced left and down in Fig. 3 (not shown in the figure).

The orbital light curves in the R′ band, which is the R band corrected for the Hα emission line contribution and in the "cont" band, which is the S band of the Vilnius photometric system (Goranskij et al., 1997; Kayumov et al., 1989) corrected for this line, are displayed in Fig. 4. The S band is centered on the Hα, its FWHM = 260 Å. The average contribution of this line to the R band is 12–13 % (Goranskij et al., 1997). The data on the eclipse of 1986 commence at phase 0.9 and terminate at phase 0.25 of the next orbital cycle. It is seen from the figure that the behaviour of the continuum flux at Hα tracks completely that of R′. The displacement by about $0\overset{m}{.}4$ corresponds to the slope of the SS 433 spectrum. The two light curves demonstrate clearly the eclipse. One can also see the flare at the beginning of eclipse 2.

Fig. 5 shows the behaviour of the Hα line flux versus the precession ($0.8 < \psi < 0.2$) and orbital phases. This figure involves all observations of the authors in the Hα (S) band which were obtained within the frames of the co-operative programmes. The data on eclipses 1 and 2 are denoted the same as in the previous figure. Two upper circles refer to the flare at the beginning of eclipse 2. The crosses, triangles and squares are used to denote observations at other orbital cycles. The flux in Hα is seen to change strongly in a narrow interval of ψ. An abrupt rise of brightness takes place from $\psi \approx 0.8$ to $\psi \approx 0$. Goranskij et al. (1987) has ironically interpreted the increase

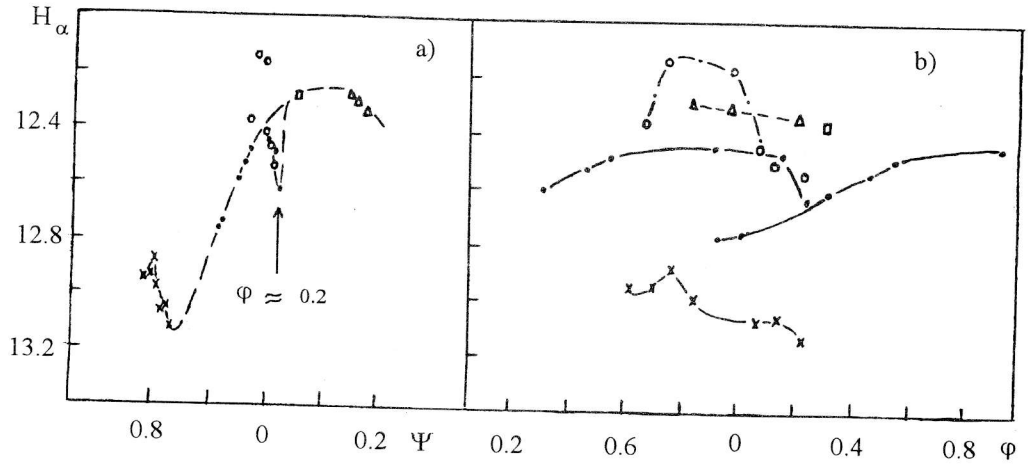

Figure 5: *The light curves in* Hα *as a function of precession (a) and orbital (b) phases.*

of the Hα flux after the orbital phase $\varphi = 0$ as the end of the orbital eclipse, whereas actually the Hα line flux was rapidly increasing (see the lower curve shown by dots in Fig. 5 b) with increasing of the precession phase in the phase interval $0.91 \leq \psi \leq 0.99$. Comparing the light curves in Figs. 5 a and 5 b one can infer that no marked variations of flux in the Hα line with the orbital phase occur, but for the orbital phases $0.1 < \varphi < 0.3$ where the eclipse is observed. The arrow on the precession curve marks the reduction of the flux due to partial eclipse at $\varphi \approx 0.2$. The amplitude of this eclipse in Hα is approximately 20 %. This decrease in Hα flux is well seen on the orbital curves only at precession phases about 0. At the adjacent precession phases the depth of eclipses is smaller or they are lost against the background of the fast precession changes in Hα flux. The precession curve of the Hα emission line variations is consistent with the average precession curve of SS 433 from (Gladyshev, 1980), but has a smaller amplitude.

3. Analysis of emission line profiles in eclipses

The spectral observations were performed at the 6 m telescope with the TV–scanner (Drabek et al., 1986). The spectral range was $\lambda\lambda 3500 - 5200$ and $5300 - 7000$, the dispersion was 1.7 – 1.8 Å/channel. In Table 1 a journal of the spectral observations is presented: Julian Date of a middle of exposure, the exposure time, the orbital period phase φ and the spectral range covered. The spectra were reduced for the non–uniformity of the photocathode sensitivity and the night–sky spectrum was subtracted. Then the spectra were reduced to absolute fluxes (in erg cm^{-2} s^{-1} Å^{-1}) with the aid of the photometry data (Fabrika et al., 1997 b). The emission lines contribute in the B and V bands no more than 2–3 %, therefore the absolute calibration of fluxes in the lines of interest He II λ 4686 and Hβ is correct enough.

The description of the SS 433 spectrum in eclipse 1 (1986) and on the dates that followed is presented in (Goranskij et al., 1987). In the spectra are seen strong emission lines Hα, Hβ, Hγ, Hδ and He I with the P Cyg type profiles, the emission line He II λ 4686, the blend of the emission lines C III, N III $\lambda_{\rm eff}$ 4644, weak emission lines Fe II, which have the profiles of type P Cyg too, and also numerous moving emission lines H$\alpha^{\pm}$, H$\beta^{\pm}$, H$\gamma^{\pm}$, Hδ^{+} and Hε^{+} of complex structure. During the eclipses no drastic change in the spectrum was noticed, no spectral lines were observed to appear or disappear either. In a middle of a primary minimum the line He II λ 4686 looks more narrow than out of eclipse by 30 % (FWHM) (Goranskij et al., 1987). The other lines show lower variations.

In eclipse 2, in the active state a variability of the He II λ 4686 line profile width and its intensity are still greater. The variability of the line profile is notable even in the spectra taken sequentially. The emission features H I and Fe II have no absorption components. For these observations the spectra of the first ($\varphi = 0.007 - 0.011$) and third ($\varphi = 0.238$) nights are of low quality (taken through the clouds), therefore the measurement accuracy of line parameters is worse than that for the spectrum of the second night ($\varphi = 0.078 - 0.084$). The phases the spectra were obtained at are indicated by the vertical bars in Fig. 1.

Table 1: *Log of spectral observations*

Spect.	JD 244...	Δt	φ	λ(Å)
16902	6583.425	47^m	0.0252	3460–5160
16903	.459	44	0.0277	3690–5390
16904	.487	31	0.0299	–
16905	.507	15	0.0314	–
16906	.521	12	0.0325	5280–7080
16907	.527	6	0.0329	–
16908	.531	5	0.0333	–
17005	6584.352	40	0.0960	3580–5280
17006	.383	40	0.0984	–
17007	.414	40	0.1008	–
17008	.436	20	0.1024	–
17009	.453	20	0.1037	–
17010	.469	20	0.1050	–
17011	.485	20	0.1062	–
17012	.501	20	0.1074	–
17013	.515	18	0.1085	5150–6950
17014	.526	6	0.1093	–
17105	6585.343	30	0.1718	3580–5280
17106	.366	30	0.1735	–
17107	.388	31	0.1752	–
17108	.413	30	0.1771	–
17109	.435	30	0.1788	–
17110	.458	30	0.1806	–
17111	.482	30	0.1824	–
17112	.506	20	0.1842	5160–6960
17204	6587.451	30	0.333	3570–5270
17205	.473	25	0.335	–
17206	.493	25	0.336	–
17207	.515	28	0.338	5150–6950
37201	7407.376		0.0088	3570–5270
37211	7408.287		0.0784	–
37212	.306		0.0798	–
37213	.322		0.0810	–
37214	.339		0.0823	–
37215	.355		0.0835	–
37302	7410.380		0.238	–

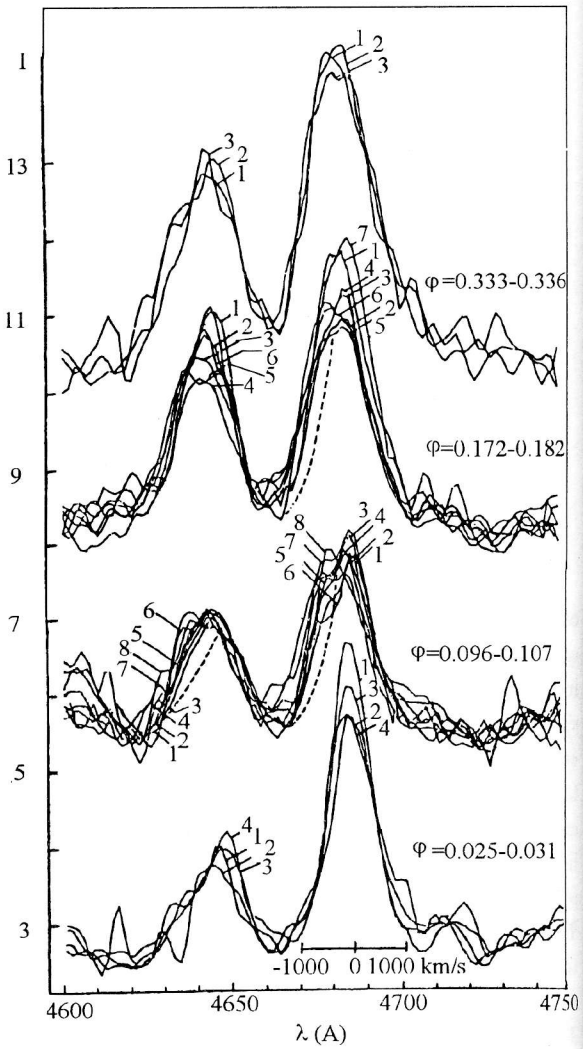

Figure 6: *The line profiles of He II λ 4686 and C III, N III λ_{eff} 4644 on June 1–5, 1986. Bottom — at phases of eclipse "bottom", top — out of eclipse. Intensity is given in* 10^{-15}ergs^{-1}cm^{-2}Å^{-1}. *The spectra of the 2nd, 3rd and 4th nights are shifted up by 1.5, 3.7, 5.3 respectively. The dashed line shows the red line wing reflection.*

The He II λ4686 line

In Figs. 6 and 7 the He II λ4686 line and the C III, N III $\lambda_{\rm eff}$ 4644 blend profiles obtained during eclipses 1 and 2, respectively are presented. The spectra obtained on the same night are superimposed to show the profile variations. For each night the spectra are consecutively numbered.

At the phases of "bottom" of eclipse 1 ($0.025 \leq \varphi \leq 0.031$) the He II profile is the most narrow and symmetrical and well approximated by Gaussian, its FWHM $\approx$ 1000 km/s. The radial velocity of the Gaussian component is V_r = 54 km/s. At the phases φ = 0.096 – 0.107 a bright blue wing appeared in the profile immediately after the second contact, which broadened the line. The Gaussian component intensity reduces at these phases by a factor of 1.5 – 2. The local peak of this component is, however, seen almost in every spectrum. On the blue side of the profile a large scatter is observed: during 20 – 40 minutes maxima and individual details of the wing appear and disappear. The fast emission variability of the

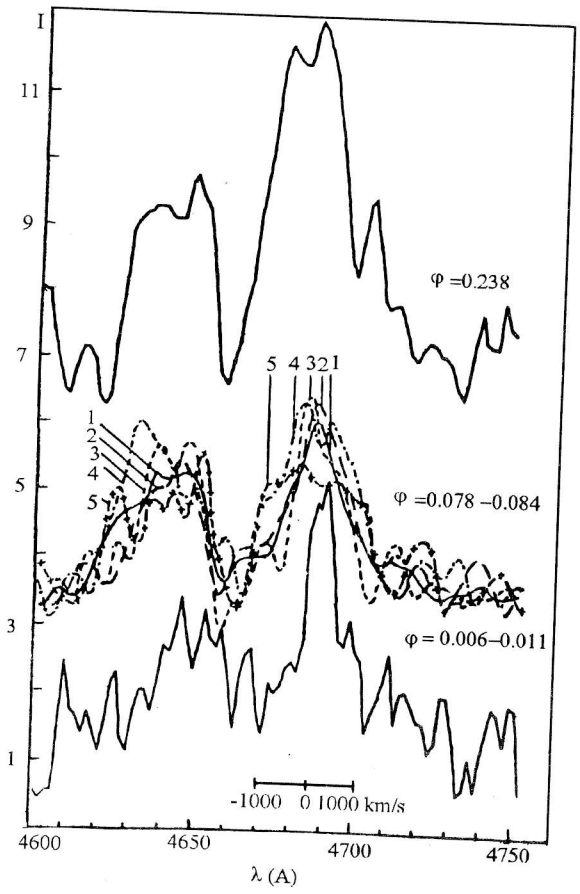

Figure 7: *The line profiles of He II λ 4686 and C III, N III* λ_{eff} *4644 on September 2–5, 1988. The spectrum of the 1st night is shifted down by 1.8, of the 3rd night – up by 1.8.*

blue wing, the appearance and disappearance of small peaks may be due to irregular outflow of matter. At the same time the position of the red part of the profile is not shifted with respect to that in eclipse. The blue wing intensity is variable and it grows from the early spectra to the late. The line profile width on this and the following nights increases with the appearance of a blue wing by 300 – 500 km/s; separate details, however, extend up to $V_r = -1500$ km/s.

In the middle of eclipse 2 the He II emission line is very narrow with the FWHM $\approx$ 700 km/s and radial velocity of the corresponding Gaussian component is about 150 km/s. On the next night the line profile is seen to broaden and the peak to shift blueward. The profile is variable both on the red and blue sides; the emission intensity in the two wings increases with time, however, as well as in eclipse 1 the blue wing is more variable. Not only the He II line is variable but also the C III, N III total profiles. The narrow Gaussian component is decreasing on the second night in the same fashion as in eclipse 1. A night later (the star being already out of eclipse) a powerful He II emission is observed. Even in active state the spectra confirm qualitatively the behaviour of the He II line profile in eclipse 1.

So, the He II line consists of two components emitted from different regions: a broad asymmetric and more variable component which is eclipsed in the middle of the primary minimum (the accretion disk centre eclipse) and a narrow one (fitted well by Gaussian) component eclipsed by the optical star at later phases.

Figs. 6 and 7 suggest that we observed a total eclipse of a small region around the base of the jet and an emergence of this region from behind the star limb. In the centre of eclipse 1 the He II line profile is narrow and very well approximated by the Gaussian. The emission region of the broad wings of the line profile is totally eclipsed at this moment. Later, on egress from eclipse, vice versa, the emission region of the narrow component is gradually obscured, and that of the broad component (connected with the central part of the accretion disk) emerges. This conclusion is completely corroborated by the dynamics of the He II line profile in the eclipse. In this eclipse, just before the contact, the variable radiation in the line wings appears and grows. We have isolated the He II line profile emitted in the disk (the broad component) by subtracting the Gaussian profile from the observed one. The radial velocities of the He II line profiles have preliminarily been corrected for orbital motion on the basis of the radial velocity curve (Fabrika, Bychkova, 1990) obtained from all the 6 m telescope data.

To estimate the relative sizes of the He II line emission regions we have made a Gauss–analysis of the night's averaged profiles. In Fig. 8 are presented the fragments of the mean eclipse 1 spectra with the lines C III, N III and He II involved; below is given the spectrum of the second night of eclipse 2 (during the 1st and 3rd nights only one spectrum a night and of not good quality has been taken). On the right from the line He II the emission line He I λ 4713 is well seen. Two relativistic emission lines are also visible in the spectra (for the identification of the spectra see Goranskij et al., 1987). From the He II line profile the Gaussian profile has been subtracted, whose approximation being done by minimizing the residual line intensity. The subtraction result is shown in Fig. 8 by dashed lines. The residual profile is readily

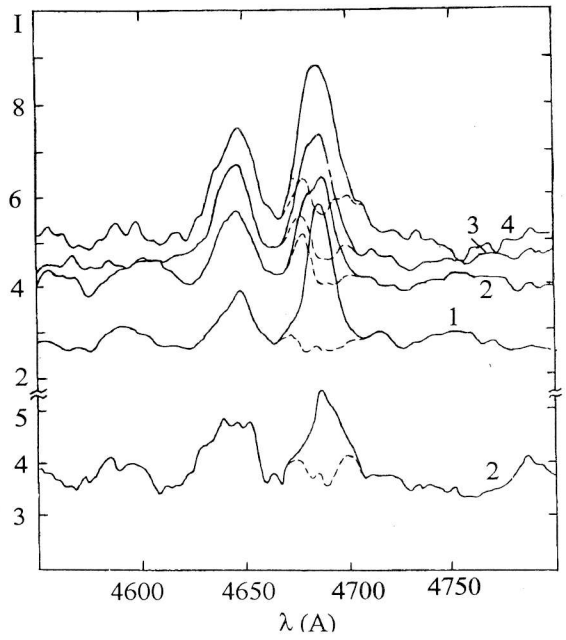

Figure 8: *The summary spectra for a night of eclipse 1 and for the 2nd night of eclipse 2. The intensity units are the same as in Fig. 6. The numbers denote a night number during eclipse. The dashed lines show the residual spectra after subtraction of Gaussian profile from the He II. The residual profiles are double-peaked.*

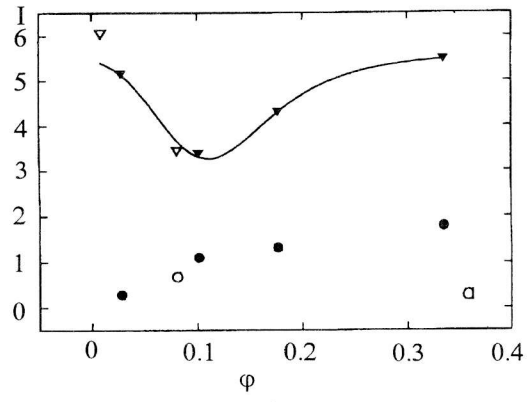

Figure 9: *He II fluxes in the Gaussian line component (triangles) and the blue component of the double-peaked profile (circles) (10^{-14}erg s^{-1}cm^{-2}) as a function of orbital phase, obtained from the average spectra. The filled symbols — eclipse 1, open — eclipse 2. The narrow Gaussian component is eclipsed at phase 0.11.*

seen to be double-peaked. On the first night of eclipse 1 the subtraction turns out to be pratically full (total eclipse of the broad He II line component by optical star). The small excess in the blue wing is about 5 % in intensity of the whole line observed. Correct approximation of the He II line profile is complicated by the presence of the He I λ 4713 line in its blue wing. The intensity of the latter is much lower than that of He II. During the second night an intensive blue wing of the broad component appeared. In the residual profiles of the next two nights the red component is pronounced too. It is less intensive than the blue one.

It is well seen in eclipse 2 (Fig. 8) that the residual He II profile is also double-peaked, but the both components are of approximately equal intensity. The fact that in the middle of the disk eclipse the line is excellently described by the narrow Gaussian profile regularizes the deblending process. This suggests that it is the Gaussian profile that should be subtracted from the profiles of this line which were obtained on the nights that followed. An argument in favour of correctness of our subtraction procedure is the regular behaviour of the parameters of the obtained Gaussian components in the eclipses (see below). Zwitter et al. (1991) have also made Gauss-analysis of the He II profile. To comply with the requirement of mimizing the residuals they isolated as many as three components, however, they failed to draw any definite coclusions on the nature of these components. Based on the analysis of this line behaviour in eclipse, we have separated two components (one of them is double-peaked) that correspond to physically separated regions.

In Fig. 9 the relationship is shown between the He II fluxes in the Gaussian component obtained (triangles), in the blue component of the double-peaked profile (circles) and the orbital phase. The line fluxes in eclipse 2 were multiplied by a coefficient 1.15 that was chosen from considerations of compatibility of the curves. It is safe to say from the figure that the region of formation of the narrow Gaussian He II component is eclipsed by the optical star but partially. The minimum intensity of the narrow component occurs at a phase of about 0.11, the eclipse depth is about 35 %. The eclipse of this emission region is, apparently, non-symmetric, the egress is flatter than the ingress.

The region where the blue peak of the broad component is produced is almost completely covered in the centre of the primary minimum and suddenly opens up in the region of the X-ray contact at the phase $\approx$ 0.09. In Fig. 10 is displayed the blue peak in-

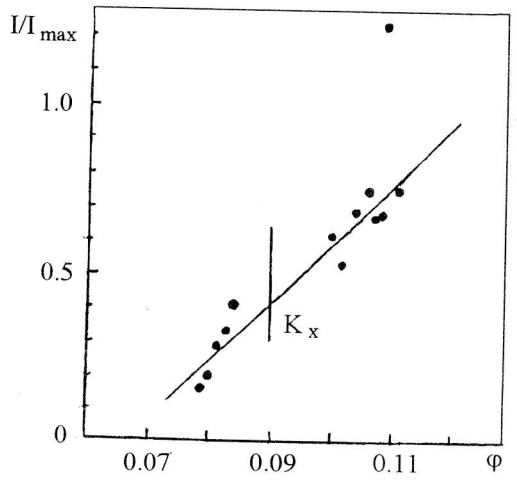

Figure 10: *Intensity of the He II λ 4686 blue component of the double-peaked profile as a function of orbital phase, obtained from the individual spectra. The average intensity out of eclipse is taken as unit.* K_X *— the phase of the last contact of the X-ray eclipse.*

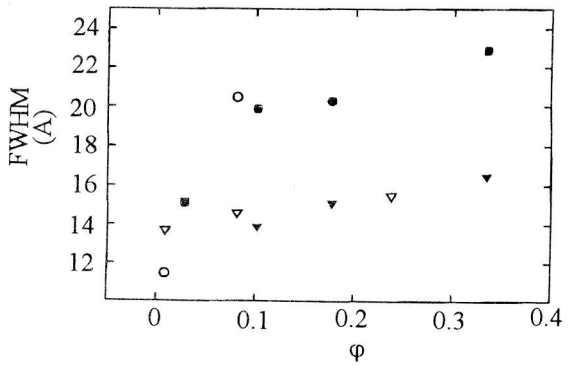

Figure 11: *Variations the He II observed profile FWHM (circles) and that of the Gaussian component (triangles). A sharp increase of the total profile width is seen at the accretion disk egress from the eclipse. Filled symbols — eclipse 1, open ones — eclipse 2.*

tensity variation versus orbital phase, which has been obtained from the individual spectra. The moment of the contact of the X-ray eclipse K_X is near the middle of the ascending branch, therefore a source of the emission He II broad component (the blue peak) is the region situated around the X-ray jet. The duration of emergence of the region from behind the limb is estimated as $0.04 \div 0.05$ of the orbital period, which determines its size to be $0.25 \div 0.30$ in units of the system components separation or $0.27 \div 0.32$ in units of the eclipsing star size.

Fig. 11 presents the variation of the total observed He II line profile width (circles) and that of the Gaussian component (triangles), which have been obtained from the average spectra. An abrupt rise in the width of the total profile from the phases of the eclipse "bottom" to the phase 0.1 is well seen, that is, the appearance of the He II line broad component. Near the centre of the eclipse the width of the total profile, as it was to be expected, coincides with the width of the narrow Gaussian component. The discrepancy between these values during the first night of eclipse 2 is caused by the low quality spectrum. The Gaussian component width of the He II profile is practically constant being, on the average, 14.9 ± 0.3 Å (950 ± 20 km/s). This indicates that the line broadening is not related to the large-scale gas motions. The width is somewhat reduced at the centre of its eclipse at phase 0.1, which is consistent with the assumption of the broadening due to electron scattering (Kopylov et al., 1989). The regular behaviour of the parameters of the isolated narrow component — the constancy of its width and the smooth intensity variation in the eclipse — suggests that the narrow component is formed in a physically and spatially independent region. This region is separated from the accretion disk centre by 40° ($\Delta\varphi \approx 0.11$). When approximating the profile by the Gaussian function we did not impose any restrictions on the function parameters. The only requirement was that the subtraction be as full as possible, without forming absorption details in the residuals. Therefore the regular behaviour of the narrow component parameters is an indication of correctness of the He II profile division we have done.

The independence of the emission regions forming the narrow and broad components is corroborated by the radial velocity analysis. In Fig. 12 the radial velocities of the Gaussian component of the He II line profiles obtained from the average spectra are shown (points and circles with crosses). The lines in the figure show fragments of the radial velocity curves of the total He II profile which were obtained from long-term observations (Fabrika, Bychkova, 1990). The solid line is the radial velocity curve plotted from all the data (half-amplitude $K = 134 \pm 20$ km/s), the dash-and-dot line is that for the precession phase interval $0.9 \leq \psi \leq 0.1$ ($K = 175 \pm 20$ km/s), the dashed line is that for the neighbouring precession phases $0.7 < \psi < 0.9$ and $0.1 < \psi < 0.25$ ($K = 79 \pm 25$ km/s). Despite the great scatter with respect to the dashed line, $\sigma \approx 40$ km/s, (however, quite ordinary for the

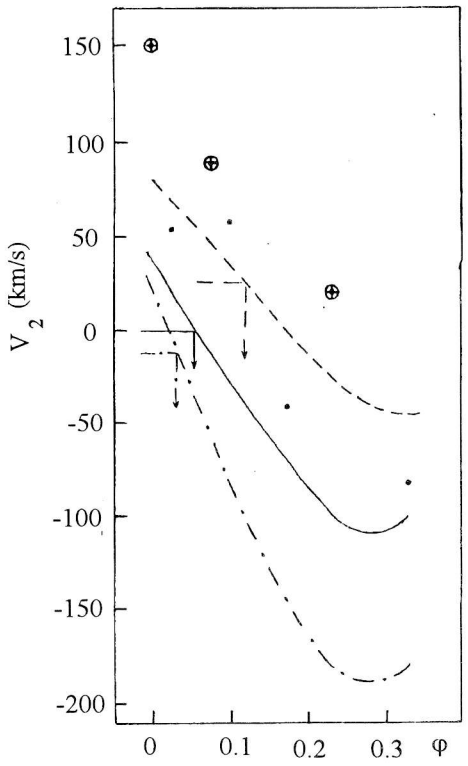

Figure 12: *The radial velocities of the narrow Gaussian component of He II. Points show the data of eclipse 1, circles with crosses — those of eclipse 2. Radial velocity curve fragments of the He II line from Fabrika and Bychkova (1990) are presented: solid line — from all the data available, dash–and–dot line — at the precession phase interval* $0.1 \leq \psi \leq 0.1$*, dashed line — at neighbouring phases of precession out of this interval.* γ*–velocities for each curve are shown also. It is seen that the radial velocity of the narrow Gaussian component corresponds to the dashed curve.*

He II radial velocities in SS 433 (Fabrika, Bychkova, 1990)), it is this line that the He II narrow component radial velocities obviously tend to. It can be stated with assurance that the narrow component's velocity does not conform to the lower curve obtained for the precession phases, which, in fact, the eclipses under study here refer to. Fabrika and Bychkova (1990) have divided the He II line into two components on the basis of its radial velocity behaviour: 1) the accretion disk component, which predominates at precession phases around $\psi \approx 0$, whose curve (dash–and–dot line in Fig. 12) intersects its γ–velocity (the mean velocity) at $\varphi \approx 0.0$, and 2) the stream component, which predominates at the adjacent precession phases, whose curve intersects its γ–velocity at $\varphi \approx 0.10$ (dashed line). The latter suggests that the region of the stream component formation must undergo an eclipse at the orbital phase $\varphi \approx 0.10$, which has just been found in the present paper. This component of He II predominates in the total profile (radial velocities) out of precession phase $0.1 < \psi < 0.9$. We have identified it with the narrow Gaussian component.

Thus herein and in the paper by Fabrika and Bychkova (1990) by independent means we have divided the He II line into two components: from the accretion disk and from the stream. The disk component is formed in its central regions (the jet bases) and undergoes practically a total eclipse at orbital phase 0. The radial velocity half–amplitude of the accretion disk orbital motion is not less than 175 km/s. The second and more intensive component is relatively narrow and symmetric. It undergoes a partial eclipse at orbital phase 0.1, so the region of its formation is shifted with respect to the line that connects the centres of the stars at $\triangle\varphi \approx 0.1$. The orbital radial velocity curve of this component (stream) is delayed relative to the accretion disk accordingly by the phase interval 0.1. The half–amplitude of the stream component radial velocity makes up 80 km/s.

The behaviour of the C III, N III blend profile follows qualitatively that of the He II line, but the compexity of the blend does not allow a simple analysis to be made. Proceeding from the ionization and excitation potentials of these lines the conclusion can be drawn that the temperature of the regions being discussed in both the accretion disk and the stream is about $(3 \div 5) \cdot 10^4$ K.

The Hβ line

The behaviour of hydrogen and He I emission lines in the eclipse is different. Figs. 13 and 14 show the profiles of the Hβ, and the weak He I λ 4922 line in eclipses 1 and 2, respectively. In the first eclipse Hβ has a profile of P Cyg type. The absorption component of Hβ extends as far as $V_r = -1500 \div -2000$ km/s. The emission line has FWHM of about 840 ± 40 km/s, i. e. similar to the width of the He II narrow Gaussian component. At phase 0.1 its width decreases (the same as in this component of He II) down to 740 km/s. The Hβ emission line in the middle of the accretion disk eclipse shows a maximal intensity measured in the continuum intensity units (see also Fabrika et al. (1997 b)). Then the

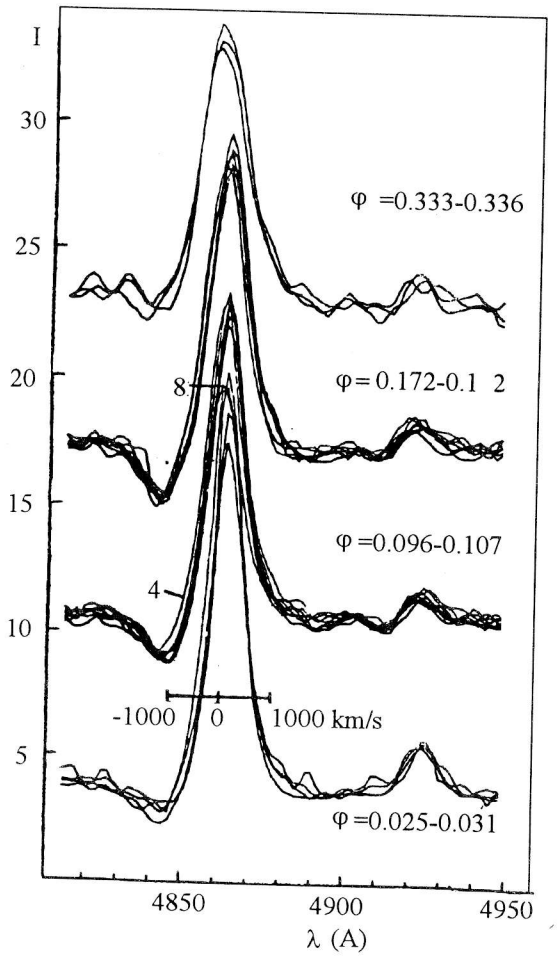

Figure 13: Hβ *and He I* λ4922 *line profiles on June 1–5, 1986. The intensity units are the same as in Fig. 6. The spectra of the 2nd, 3rd, and 4th nights are shifted up by 5.2, 10.5, and 16.0 units, respectively.*

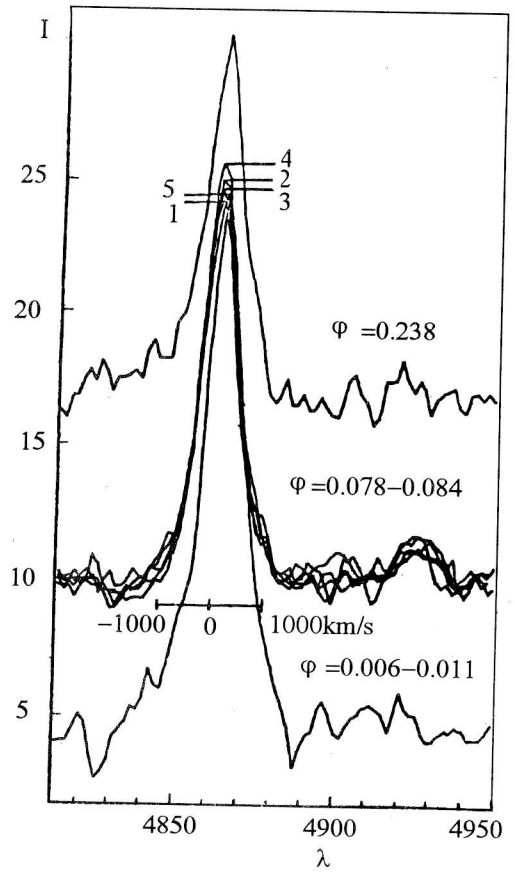

Figure 14: Hβ *and He I* λ4922 *line profiles on September 1–5, 1988. The intensity units are the same as in Fig. 6. The spectra of the 2nd, and 3rd nights are shifted up by 5.2, 10.5, respectively.*

intensity drops, that is, the behaviour of Hβ intensity also resembles that of the narrow component of He II. At the centre of the eclipse the absorption line in the blue wing is conspicuous, its equivalent width is about 3 Å. During the next 2 nights on the egress branch the intensity of the absorption line increases a little, however, after egress of the accretion disk from the eclipse the absorption line intensity sharply drops. The profiles change only slightly during the night. Analysis of the absorption components of hydrogen and He I lines in more details are presented in Fabrika et al. (1997 a, b).

In the 2nd eclipse (active state) in the place of the absorption component a weak blue emission wing is seen, which remains in the middle of the eclipse. Note, that observations of the bright blue wing in the Hβ emission line have been mentioned by Filippenko et al. (1986). On the last night of this eclipse a weak line Hδ^+ appears in the blue wing of Hβ. The same as in the 1st eclipse Hβ has an intensity maximum in the middle of the eclipse, then it is gradually getting weaker at phase 0.25. However, in the 2nd eclipse the intensity of Hβ was by about 30 % higher than at the same phases of eclipse 1.

Kopylov et al. (1989) have suspected an eclipse in Hβ and Hγ at the orbital phase $\varphi \approx 0.25$. This effect could well be expected since the radial velocity curves of hydrogen lines intersect their γ–velocity curve from "+" to "–" exactly at phase 0.25 (Crampton, Hutchings, 1981; Kopylov et al., 1989). The data of the present paper are consistent with the conclusion drawn by Kopylov et al. (1989): the intensity of Hβ decreases when the orbital phase changes from 0.0 to 0.25. The light curves of the Hα line (Fig. 5) also

confirm the inference that hydrogen lines are eclipsed at the orbital phases 0.1 – 0.3.

Thus, from both the line width and the behaviour of its intensity versus orbital phase the Hβ line is quite similar to the narrow component of He II. The radial velocities of these two lines are similar too (see the Hβ radial velocity curves obtained by Crampton, Hutchings (1981); Kopylov et al. (1989); Fabrika et al. (1997 a)). A detailed analysis of the behaviour of stationary hydrogen and He I lines in the primary minima will be published elsewhere.

4. Discussion

The observed occultation of the blue peak of the He II profile broad component and emergence of the region emitting in this component from behind the limb at the phase $\varphi \approx 0.09$ permits this radiation to be referred to the vicinity of the jet bases. By analogy with X–ray jets (Brinkmann et al., 1989) we propose a model of hot gas cocoons coaxial with the jets, which explains the peculiarities of the hot source eclipse. The size of the blue He II component formation region determined from the duration of its egress from eclipse (Fig. 10) is $0.25 \div 0.30$ a (a is the distance between the system's components). The size of the eclipsed region of the X–ray radiation (Fig. 10) is about 0.20 a. The eclipsing star's diameter is then ≈ 0.94 a or somewhat larger. The region of He II formation can be stated to be larger than that of hard radiation. The centres of the two regions are likely to be coincident. Our observations combined with the X–ray data confirm the idea of a hot cocoon around the relativistic jet in the region of its emergence from under the photosphere of the accretion disk. Across the cocoon there is a considerable temperature gradient, cooling outward from $\sim 10^8$ K in the X–ray region to $\approx 5 \cdot 10^4$ K in the He II region. This cocoon is located on the jet's axis (of the accretion disk axis) and separated from the relativistic star by a distance no greater than the star's radius, 0.5 a, which follows from the condition of its total eclipse.

When discussing the eclipse of the accretion disk in SS 433 one should be aware that it is not the disk itself that is observed. The wind from the surface of the supercritical disk (Shakura, Sunyaev, 1973) forms an envelope which shields from the observer the central parts of the disk or the entire disk, depending on mass supplied to it. We fail to furnish an example of direct observational evidence of accretion disk in SS 433 (see, however, Filippenko et al., (1986)). Even the well–known precession modulation of the SS 433 brightness (Gladyshev et al., 1987) can be understood within the frames of the model of precession motion of the hot spots–funnels at the bases of the jet egress on the photosphere of the wind outflowing from the disk (Lipunov, Shakura, 1982; Fabrika, 1984). The photosphere radius is about 10^{12} cm.

In the spectrum of SS 433 Filippenko et al. (1988) have detected double–peaked profiles in Pachen lines. The distance between the peaks is $\triangle V \approx 300$ km/s. The authors have assumed that the double–peaked Pachen lines are formed in the accretion disk. With the Keplerian rotation velocity of gas in the region of Pachen line formation $\triangle V / 2 \approx 150$ km/s for reasonable mass values of the compact star, $1 \div 5$ $M_\odot$, the radius of the disk turns out to be $6 \cdot 10^{11} \div 3 \cdot 10^{12}$ cm. There is, however, another interpretation (see Fabrika, 1993), that these lines may well be formed in the excretion disk — in the gas escaping from the system through the libration point L_2 located behind the ralativistic component.

We have seen that the part of the He II line profile that remains after subtracting the Gaussian component is formed in the region surrounding the relativistic component, and this profile is double–peaked. Here the peaks are separated by about $\triangle V \approx 1500$ km/s. This profile can not belong to a line emitted in the disk. Indeed, with the Keplerian velocity $\triangle V / 2 \approx 750$ km/s for the same masses of the compact star, $(1 \div 5)$ $M_\odot$, the disk size in the He II line is equal to $2 \cdot 10^{10} \div 10^{11}$ cm. The duration time of egress of such a disk from eclipse does not exceed 2 hours, whereas egress of the broad He II component is observed to last not less than one day (Fig. 8).

The double–peaked profile of this line may be due to asymmetry of the wind outflow as two opposite cocoons around the bases of both jets. According to the precession phase the orientation of the jets and the conditions of eclipses of the blue and red cocoon vary. In Fig. 8, in particular, it is seen that in eclipse 1 (precession phase 0.92) the red wing of the He II profile is observed to appear not earlier than the third night of the eclipse, while in eclipse 2 (precession phase 0.0) the both wings of the line profile are of approximately equal intensity and appear as early as the second night of the eclipse. The gas outflow velocity in these cocoons ("He II jets") is about $V(\text{He II}) = (\triangle V / 2) / \cos 59° \approx 1500$ km/s. Besides, we see that the opposite cocoon emitting in the red wing of the line is not eclipsed by the accretion disk body, i. e. in projection onto the sky plane the dis-

tance between the disk centre and the cocoon location is over the disk radius. Alternatively this distance is less than the radius of the optical star since we observe both wings of the broad component of He II totally eclipsed. This suggests that the star size is larger than the projection of the disk onto the picture plane.

The narrow component of He II and the total Hβ line are similar and behave themselves in eclipse in a different way: they are not completely weaken, approximately by 35 % in the case of He II and about 15 % for Hβ. The eclipse occurs at the phases $\varphi = 0.1$ in He II and $\varphi \approx 0.1 \div 0.25$ in Hβ (see also Fabrika et al., 1997 b). The eclipse in Hα is also partial, about 20 % of the line flux is eclipsed, Hα is eclipsed at $\varphi \approx 0.2$. Emission in these lines is originated far from the relativitic component, at a distance not less than 0.6 a. It can be easily found that if these lines are formed at the place of contact of the accretion stream and the disk edge, i. e. the accretion disk radius is 0.6 a, then with involvement of the known mass function of SS 433 (Fabrika, Bychkova, 1990) the masses of the two stars of the system appear to be excessively large. This suggests that the narrow component of He II and the hydrogen lines are emitted far from the accretion disk. The size of the region of formation of this He II line component determined from the duration of its ingress into eclipse (Fig. 9) is ≈ 0.4 a. Besides we can see that the phase of the last contact for the corresponding line decreases with increasing ionization potential of the element. This indicates that as the gas stream is approaching the disk the gas temperature is rising.

Apparently, the narrow component of He II and the hydrogen lines are produced in the accretion stream directed to the disk. The coolest parts of the stream, in which the hydrogen lines are basically emitted, are located in the regions being in a superior conjunction at phases 0.1 – 0.3, the radial velocity half–amplitudes of these regions is about 70 – 80 km/s. The hydrogen lines that are formed in these regions are strongly distorted by absorption and displaced redward (Crampton, Hutchings, 1981; Kopylov et al., 1989; Fabrika et al., 1997 b). The hotter parts of the stream, where the He II line component is formed, are in a superior conjunction and eclipsed at the orbital phases ≈ 0.1, their radial velocity half–amplitude is 80 km/s, they are also redward shifted (Fig.12 in Fabrika, Bychkova, 1990). Fabrika et al. (1997 a) have investigated the behaviour of radial velocities of H I, He I and He II with precession period phase and concluded the shift of these lines redward to be caused by the gas absorption in the wind outflowing from the accretion disk.

For helium to be effectively ionized in a shock wave, the stream velocity must be about 50 – 100 km/s. It is an important fact that the line width emitted in the strea is FWHM $\approx$ 1000 km/s, m. The virial velocity in the system is about 200 km/s, and the binary system gas can not move at a higher velocity. The stream emission lines may be broadened only by electron scattering, which is confirmed by approximate constancy of the narrow He II component. Kopylov et al. (1989) have shown that at a rate of overflowing of $\sim 10^{-4}\,M_\odot/y$ the optical thickness of the stream for the electron scattering is quite sufficient for the lines formed in the stream to be broadened. In this interpretation the accretion stream is eclipsed partially by the optical star in the phase range $\varphi \approx 0.1 \div 0.3$. We do not observe the stream lines to disappear completely, which suggests that this region is largely extended.

Acknowledgements. The authors wish to thank G. P. Chernova, N. K. Mitkulov and K. V. Tarasov for help in observations at the Sanglok Observatory. The work was supported by grant from the Programme "Astronomy" of RAS and grant from RFBR 96-02-16396. The authors express their gratitude to ESO for support through C&EE Programme grant A-02021.

References

Brinkmann W., Kawai N., Matsuoka M.: 1989, Astron. Astrophys., **218**, 13

Crampton D., Hutchings J.B., 1981, Astron. J., **251**, 604

Dolan J.F., Boyd P.T., Fabrika S., Tapia S., Bychkov V., Panferov A., Nelson M.J., Percival J.W., van Citters G.W., Taylor D.C., Taylor M.J., 1997, Astron. Astrophys., in press

Drabek S.V., Kopylov I.M., Somov N.N., Somova T.A., 1986, Astrofiz. Issled. (Izv. SAO), **22**, 64

Fabrika S.N., 1984, Pis'ma Astron. Zh., **10**, 42

Fabrika S.N., Bychkova L.V., 1990, Astron. Astrophys., **240**, 5

Fabrika S.N., 1993, Mon. Not. R. Astron. Soc., **261**, 241

Fabrika S.N., Bychkova L.V., Panferov A.A., 1997 a, Bull. Spec. Astrophys. Obs., **43**, (this issue), 75

Fabrika S.N., Goranskij V.P., Rakhimov V.Yu., Panferov A.A.,Bychkova L.V., Irsmambetova T.R., Shugarov S.A., Manirov T.K., Borisov G.V., 1997 b, Bull. Spec. Astrophys. Obs., **43**, (this issue), 109

Filippenko A.V., Romani R.W., Sargent W.L.W., Brandford R.D., 1988, Astron. J., **96**, 242

Gladyshev S.A., 1980, Astron. Tsirk. N 1138, 1

Gladyshev S.A., Goranskij V.P., Cherepashchuk A.M., 1983, Pis'ma Astron. Zh., **9**, 3

Gladyshev S.A., Goranskij V.P., Cherepashchuk A.M., 1987, Astron. Zh., **67**, 1037

Goranskij V.P., Kopylov I.M., Rakhimov V.Yu., Borisov N.V., Bychkova L.V., Fabrika S.N., Chernova G.P., 1987, Soobshch. Spets. Astrofiz. Obs., **52**, 5

Goranskij V.P., Fabrika S.N., Rakhimov V.Yu., Panferov A.A., Belov A.N., Bychkova L.V., 1997, Astron. Zh., in press

Kayumov V.V., Kisilev N.N., Pushnin P.A., Rakhimov V.Yu., Siklitskij V.I., Tarasov K.V., Chernova G.P., 1989, Bull. Astrofiz. Inst. Tadzhikistan AS, **78**, 10

Kawai N., Matsuoka M., Pan H.C., Stewart G.C., 1989, Publ. Astr. Soc. Pacific, **41**, 491

Kopylov I.M., Bychkova L.V., Fabrika S.N., Kumajgorodskaya R.N., Somova T.A., 1989, Pis'ma Astron. Zh., **15**, 1092

Lipunov V.M., Shakura N.I., 1982, Astron. Zh., **59**, 631

Shakura N.I., 1972, Astron. J., **49**, 921

Shakura N.I., Sunyaev R.A., 1973, Astron. Astrophys., **24**, 337

Shklovskij I.S., 1981, Astron. Zh., **25**, 315

Van den Heuvel E.P.J., Ostriker J.P., Peterson J.A., 1980, Astron. and Astrophys. Lett., **81**, L. 7

Van den Heuvel E.P.J., 1981, Vistas Astron, **25**, 95

Zwitter T., Calvani M., D'Odorico S., 1991, Astron. Astrophys., **251**, 92